

Plasmonics Enhanced Nano Composite PANI-MWNTS /Gold Particles/ Si Solar Cells

S. AbdulAmohsin

Physics and Astronomy Department, University of Arkansas at Little Rock, AR 72204, USA
Email: Smabdulalmoh@ualr.edu

ABSTRACT

We developed an organic-inorganic solar cell configuration based on nanocomposite Polyaniline-Multi Walled Carbon Nanotubes /gold particles/ Si, and the PV performance was compared between in presence or absence of plasmonics phenomena by depositing gold nanoparticles on n-type Si and deposited PANI-MWNTs layer on the top of n-type Si substrate. The gold particles deposited by atomic layer deposition on the top of n-Si, significantly increase the voltage and fill factor relative to devices without gold particles. The efficiency and fill factor of the solar cell with gold particles are (0.28%, 0.311) higher than solar cell without using plasmonics phenomena (0.073, 0.275).

تحسين الاداء بلازميا للخلية الشمسية

الخلاصة

تم تطوير الخلية الشمسية (عضوية – لاعضوية) باستخدام المركب الثانوي بولي انيلين لنابيب الكربون النانوية/ جسيمات الذهب / سيكلون. فعالية (pv) تم دراستها بوجود وعدم وجود ظاهرة (plasmonics). ترسيب جسيمات النانوية للذهب على سليكون نوع n-type و ترسيب (PANI-MWCNTs) فوق السيلكون نوع (n-type). ترسيب جسيمات الذهب فوق سليكون (n-type) ادى لزيادة قيمة الفلوتية وعامل الشغل مقارنة بعدم وجودها. كفاءة الخلية الشمسية بوجود جسيمات الذهب بوجود ظاهره (plasmonics) ازادت بنسبة (0.28 – 0.311%)

INTRODUCTION

Organic/inorganic heterostructures solar cells have been studied by various groups in the past. Among those studies, there were only very little reports on PANI-MWNTs/n-type amorphous silicon [1].

Donor-acceptor solar cells convert sunlight to electrical power by splitting photo generated excitons across an interface between an electron donor and an electron acceptor material [2]. The efficiency of a solar cell based on exciton dissociation at a donor-acceptor interface is efficiency = $FF * I_{sc} * V_{oc} / P_{in}$. The power conversion efficiency is limited because the exciton diffusion length of the donor material is typically significantly shorter than its absorption length, This problem has been addressed in

organic-inorganic hybrid solar cells by adopting a p-n heterojunction, in which the donor and acceptor phases are contact to form junction such that the majority of excitons are generated within a diffusion length of the interface[4,3]. The respectable efficiencies of certain p-n heterojunction cells may soon enable the marketing of these devices as low-cost alternatives to conventional thin-film photovoltaic.

Nanocomposite Polymer – Carbon nanotube -inorganic hybrid solar cells are interest because they support the conductive polymer which has low conductivity by MWNTs to increase the conductivity of organic semiconductors, in addition to improve the nanocomposite materials mechanically, electrically and electronically to be high electron mobility [5]. Hole-conducting polymers have been combined with a wide range of inorganic nanomaterial, including CdSe quantum dots, rods, tetrapods and hyper-branched colloids, ZnO [6-9] TiO₂ and Si rods, tetrapods and hyper-branched colloids, TiO₂ and Si [5,10-17] and PbS, PbSe, CuInS₂, and CuInSe₂ nanoparticles [18-22] [25-27]. Several theoretical studies conclude that the particles of gold should complement the polymer as a light trapper in addition to make plasmonic solar cells using gold particles. N-type Si /gold /PANI-MWNTs, use MWNTs 5wt% to improve mechanical, electrical properties for PANI [30] [28, 29] the gold nanoparticle should complement the polymer as a light absorber as Plasmon. Over the past several years, we have developed gold nanoparticle arrays suitable for both polymer-inorganic cells and dye-sensitized cells. Several groups have built polymer-inorganic cells from their own gold particle arrays [30-33].

To increase the efficiency for organic-inorganic solar cell, plasmonics phenomena can be used to trap light inside to increase the absorbance. In conventional thick Si solar cells, light trapping is achieved using gold particles the Si surface that cause scattering of light into the solar cell over a large angular range, thereby increasing the effective path length in the cell. These gold particle support surface plasmons: excitation of the conduction electrons at the interface between a metal and dielectric materials.

The Plasmon excited in metal nanoparticles and surface Plasmon polarizations propagating at the metal /semiconductor interface are of interest. In this work, we integrate gold metal nanoparticles, which exhibit intense absorption due to surface Plasmon resonance in the visible region of the spectrum. Used hydrothermally grown gold nano particles arrays on Si The device, Light can be concentrated and folded into a thin semiconductor layer, the modulation increasing the absorption.

EXPERIMENTAL SECTION

2.1 MWNTs used in this work were prepared by chemical vapor deposition of acetylene on a bimetallic Fe-Co (2.5:2.5wt %) /MgO catalytic system as described elsewhere [1]. The as-produced MWNTs were put in a furnace at 350 °C for 2 hrs to burn amorphous carbon, and then purified by refluxing in HCl and in deionized water respectively for 24 hrs. Finally, the obtained materials were dried at 100 °C for 24 hrs. The purity level of the final product was above 97%. The purified MWNTs were dispersed in Dimethylformamide (DMF, 0.2 mg/ml) and airbrushed onto ITO-coated glass slides with a surface area of 1.5 cm².

Polyaniline was synthesized by oxidative polymerization of the aniline monomer in the presence of Ammonium Per sulfate at 0 °C temperature where surround the container

by Ice. Aniline monomer was distilled twice under reduced pressure before use. The polyaniline was synthesized by dissolving 0.1 M of aniline monomer in a 1 M sulfuric acid, with 10 gram of Ammonium Persulfate, Aniline, and other organic solvents were purchased from Sigma Aldrich. Where all was placed in a 250 mL Becker. Aniline (4 ml (0.1 M)) was added to the suspension via syringe and the solution was stirred for 6 h under at 0°C temperature. The blue mixture was filtered, washed by DI water and followed by methanol, 10 mg and 5 wt % loading MWNTs dissolve them in 1 ml Chlorophorm then using bath stirrer for 30 min then magnetic bare for 24 hour at 60 °C to dispersing MWNTs with PANI finally using spin counter for 2000 rpm to get uniform thin film of nanocomposite on the top of n-Silicon wafer for measurements like UV, IR, Raman spectroscopy, and Photoluminesces spectroscopy. Figure (1) explains our Device solar cells

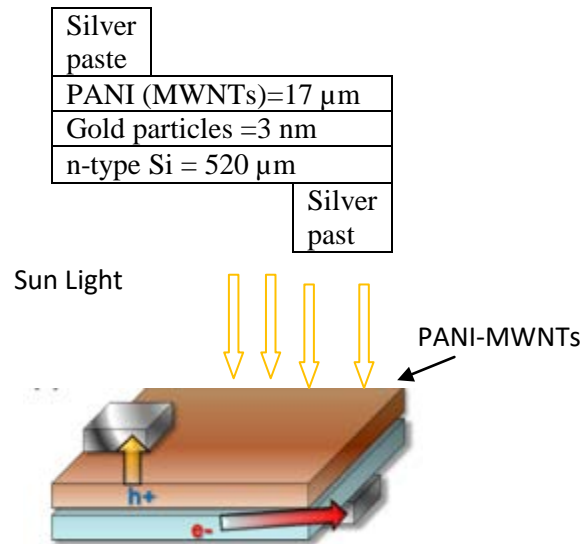


Figure (1) Schematic diagram of Organic-inorganic hybrid solar cells.

Fabrication of Si/gold /PANI-MWNTs devices

Etching n-type Si-wafer ($1 \times 1.5 \text{ cm}^2$) by HF for 17 seconds then washed by deionized water for 5 min. Use evaporation technique to deposit gold particles on the top of nSi, deposit the nanocomposite PANI-MWNTs, followed by fabrication of electrode by using silver paint .

RESULTS AND DISCUSSION

Characterization of MWNTs, PANI and the PANI-MWNTs composites

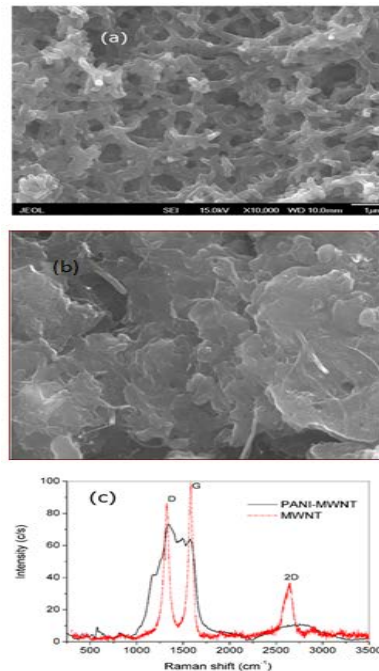


Figure (2) The SEM image of PANI (a) and MWNT-PANI composite (b) and Raman spectra of the pristine MWNTs and MWNT-PANI composite (c). The inset in (b) is an SEM image of pristine MWNTs.

A typical SEM image of a PANI thin film is shown in Figure (2a). After polymerization, PANI on ITO glass shows typical rod-like structures of 100-200 nm in diameter. However, the MWNT-PANI composite exhibits distinguished surface morphologies as shown in Figure (2b). The rod-like structures disappear in the composite. Some of the MWNTs embedded in the PANI film are visible under SEM. The representative Raman spectra of the MWNTs and the MWNT-PANI composite are shown in Figure (2c). MWNT features several characteristic bands including D ($1305\text{-}1330\text{ cm}^{-1}$), G ($1500\text{-}1605\text{ cm}^{-1}$), and 2D ($2450\text{-}2650\text{ cm}^{-1}$) bands. Both D band associated with defects and impurities and G band of the stretching mode of the carbon-carbon bonds were observed in the MWNTs. The second-order 2D-band present in the Raman spectra of various sp^2 carbon materials is generally much more intense than the disorder-induced D-band. This is due to the fact that the 2D-band is symmetry-allowed by momentum conservation requirements, whereas the disorder-induced D-band only appears when there is a breakdown in the in-plane translational symmetry [34]. After wrapped with PANI, the 2D intensity significantly decreased. Additionally, several new

peaks appear at 1178, 1258, 1502 cm^{-1} . The band at 1485 cm^{-1} has been assigned to an in-plane deformation of the C–C bond of the quinoid ring of the doped PANI [35]. Therefore, this pronounced decrease gives evidence that a site-selective interaction between the quinoid ring of the doped polymer and the nanotubes occurs as a consequence of the in-situ polymerization.

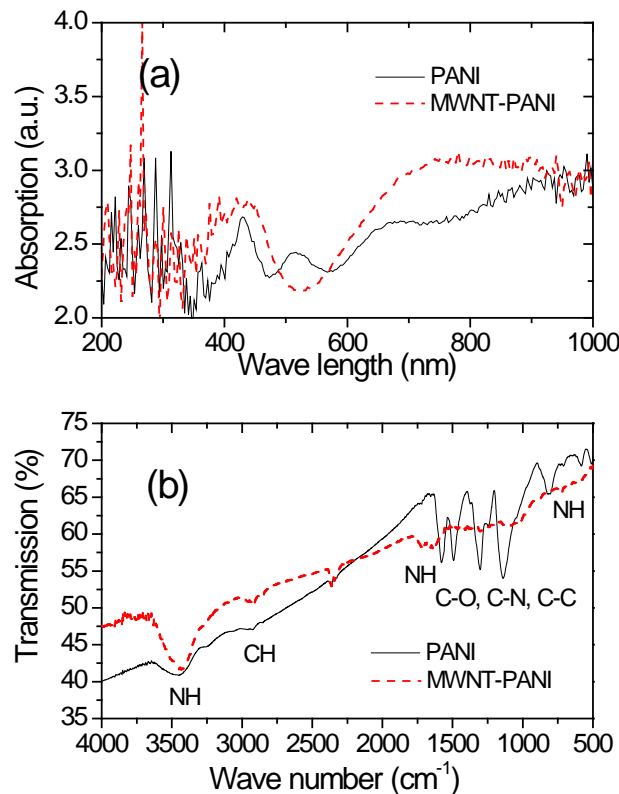


Figure (3a) Optical absorption spectra and (b) the FTIR spectra of PANI and the MWNT-PANI composite.

The UV-Vis absorption spectra of the pristine PANI and the MWNT-PANI composite are shown in Figure (3a). The pristine PANI demonstrates three strong absorption peaks around 430, 520 and 670 nm. The absorptions around 430 and 520 nm correspond to the π - π^* transitions in the benzenoid rings, while the band at 670 nm is usually ascribed to the absorption of excitons locating in the quinoid ring [36]. The peak around 290 nm represents the π - π^* electron orbital transition along the backbone of the PANI chains. Interestingly the absorption at 520 nm was quenched in the MWNT-PANI composite, indicating a strong interaction between PANI chains and MWNT walls through wrapping.

The FTIR spectra of both PANI and the MWNT-PANI composite were recorded in the region 4000 cm^{-1} - 200 cm^{-1} (Figure.3b). The formation of PANI was revealed by the

absorption bands at 3460, 1603, 1179, 1124 and 834 cm^{-1} , which were attributed to the vibrations of N-H, -C=C- , Ph-NH, Ph-NH-Ph, and C-N in the aniline unit [37]. The broad peak at 3440 cm^{-1} corresponding to -NH_2 stretching and the peak observed around 2925 cm^{-1} due to C-H stretching.[38]The absorptions at 1716 and 1637 cm^{-1} are attributed to the C=C stretching mode of the benzene rings and vibration of quinone rings [39,40]. The peak at 1303 cm^{-1} is due to the C-N stretching of the polymer. The strongest band observed near 1100 cm^{-1} and that at 1235 cm^{-1} are respectively due to C-C stretching and C-C twisting of the alkyl chain [41].The peak near 800 cm^{-1} is due to the N-H out-of-plane bending mode. All absorption peaks below 1500 cm^{-1} are much weaker in MWNT-PANI composite than in PANI, indicating the strong interaction between PANI Chain and the wall of MWNTs. Thus, the FTIR spectral measurements confirm the formation of polyaniline on the wall of MWNTs through the electrochemical polymerization process.

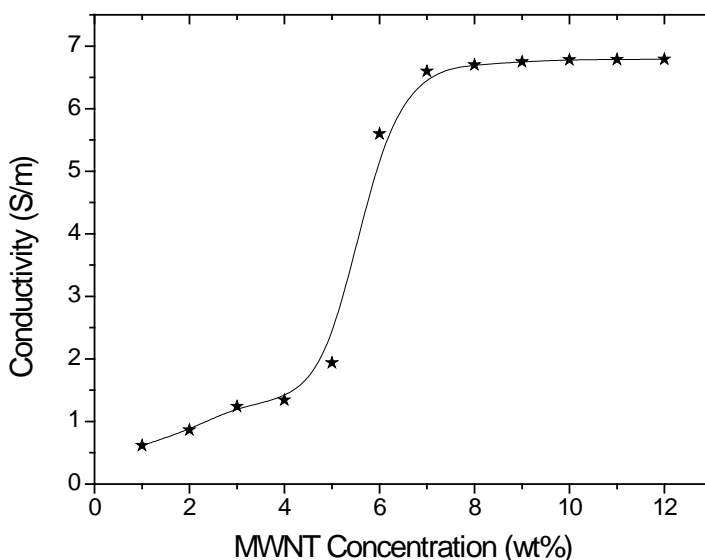


Figure (4) Effect of MWNT content on the conductivity of MWNT-PANI nanocomposites.

Figure (4) shows the effect of the MWNT content on the conductivity of the MWNT-PANI nanocomposite. One can see that the conductivity of the nanocomposite increases as the amount of MWNTs was increased. The sharp increase in the conductivity value occurs at the MWNT contents higher than 5%. The conductivity of the MWNT-PANI composite with 6% MWNTs has been increased by about a fact of 12 as compared with the pristine PANI, which indicates that the MWNT-PANI nanocomposite obtained by in-situ polymerization can significantly improve the material's conductivity. The observed changes in conductivity at different MWNT concentrations can be explained by a percolation mechanism. The conductivity is dominated by the PANI matrix when MWNT

content is below 5 wt. % in the nanocomposite at which the percolation among MWNTs starts to take over the electronic transport. Saturation in conductivity can be reached, as the MWNT content is higher than 7 wt. % where the MWNTs dominate the electrical transport. It is known that the percolation threshold depends on many parameters like nanotube type, synthesis method, tube size, and polymer type and dispersion method. [41] Studies have shown that the percolation threshold of PANI and single-walled carbon nanotube (SWNT) nanocomposite [42] is around 0.3 wt. % of SWNT concentration. A threshold of 4 wt. % for unfilled MWNT-PANI has been reported [43]. In a similar composite of MWNT with polypyrrole, the percolation threshold was estimated to be between 15 and 20 wt. % nanotubes [44]. A recent report has pointed out that it is hard to observe a sharp percolation threshold in the nanocomposite because the conduction through PANI itself smears a sudden onset of conductivity change [45].

The stability of the MWNT-PANI composites in terms of their conductivity was also investigated by annealing the samples at 100 °C in air for different times. Figure.4 shows the measured conductivity as a function of annealing time for the composite of 6% MWNTs. It was found that the initial annealing for less than 30 min improves the conductivity. However, a prolonged annealing up to 60 min causes the composite to lose its conductivity. The MWNTs embedded inside the PANI film should be stable enough to maintain their intrinsic conductivity at the annealing temperature. The oxidation of PANI itself and at the interface between PANI and MWNTs may take place and is believed to result in the loss of conductivity in the films. Effects of annealing on n-Si/MWNT-PANI solar cells were also investigated.

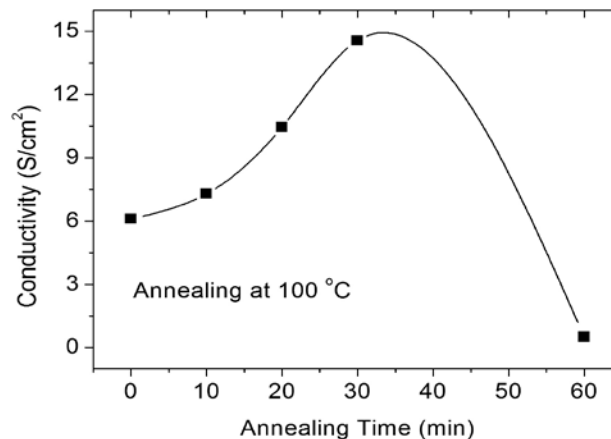


Figure (5) Conductivity of a MWNT-PANI thin film with 6% MWNTs as a function of annealing time. The annealing was performed at 100 °C in air. The solid line is used as a guide for eyes.

(1) Morphology - AFM and SEM images

For taking picture deep insight in to the case, AFM images are taken to find out what happen to the PANI-MWNTs nanocomposite. From the image Figure (6) we can find the sharp edge of MWNTs thin film it is primarily indicated that PANI is coated or

deposited on the MWNTs in to the sight film and each MWNT is coated by a certain amount of PANI.

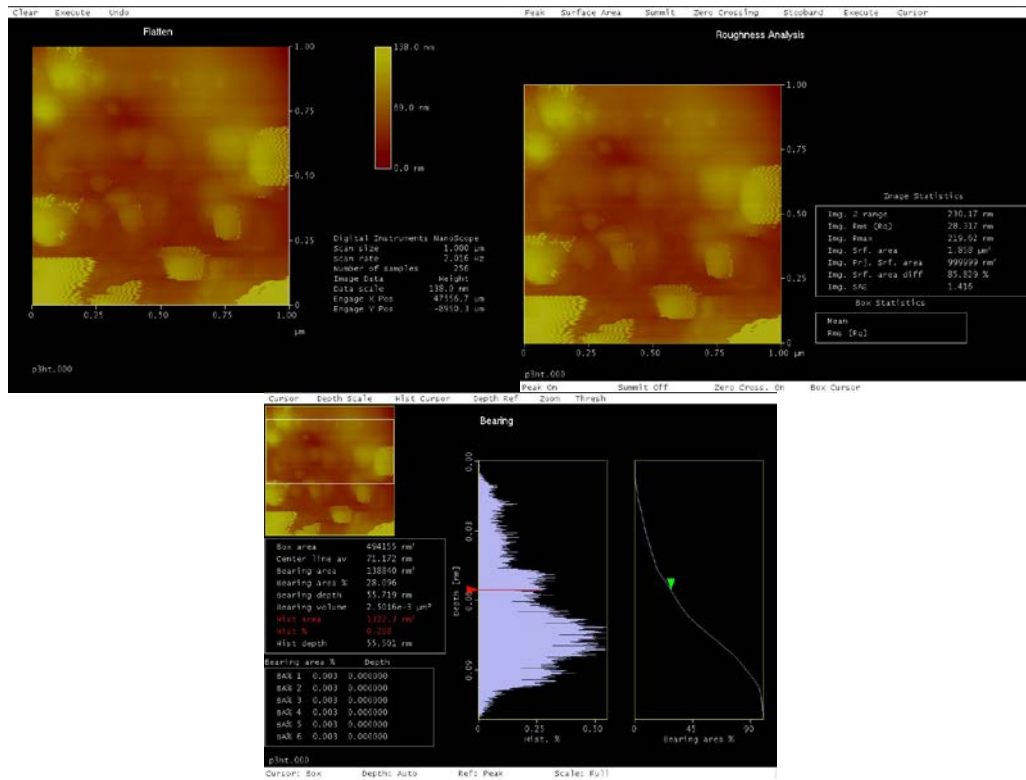


Figure (6) AFM images of PANI-MWNTs nanocomposites.

(1)PV performance of the device

Recently, PANI has been successfully used as a whole conductor material to fabricate the solid- state dye –sensitized TiO₂ solar cells [45]. Therefore, we expect the junction of PANI-MWNTs would behave as a p-n heterojunction and form a rectifying contact. The I-V characteristic for both design explain in the Figure (7) The I-V characteristic of S/Pani with and without gold for enhancing the light absorption in the thin film and organic based solar cells is called plasmonic solar cells by using metal nanoparticle.

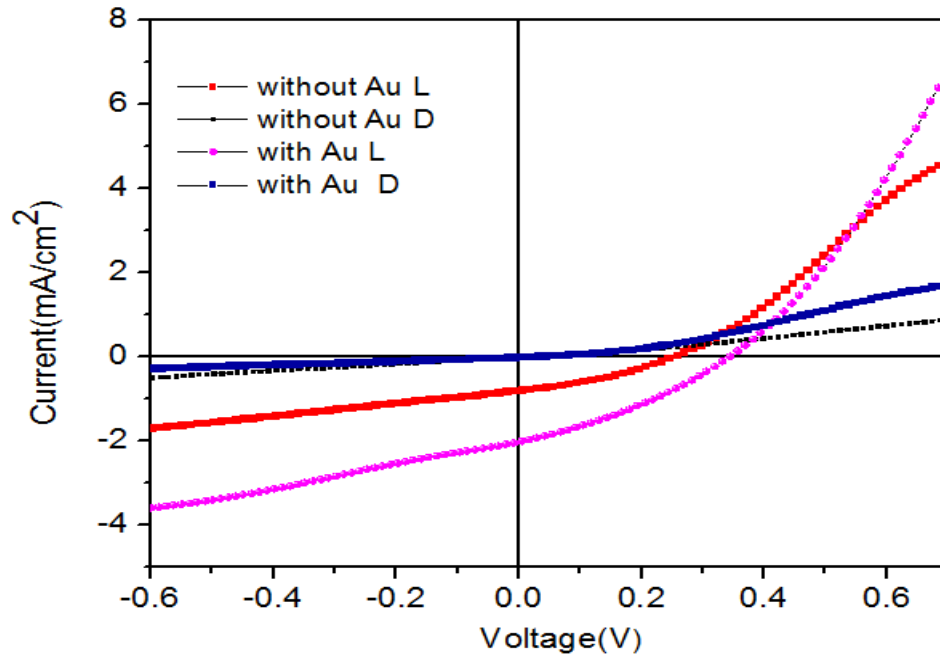


Figure (7) The I-V characteristic of the (nSi/ gold/PANI-MWNTs and (nSi/PANI-MWNTs)).

The current density voltage (J-V) characteristic of the device under illumination of simulated solar light shows a short-circuit photocurrent density (J_{sc}) of 2.02 mA/cm^2 with an open-circuit Voltage (V_{oc}) of 0.34 V for (Si/ (gold)/PANI-MWNTs) device, calculated filling factor (FF) of 0.31179 , and an overall power-conversion efficiency (PCE) of 0.28% and for the sample Si/ PANI-MWNTs which is without plasmonic effect. Figure (6) explain solar light shows a short-circuit photocurrent density (J_{sc}) of 0.8213 mA/cm^2 with an open -circuit Voltage (V_{oc}) of 0.25 V calculated filling factor (FF) of 0.275 , and an overall power -conversion (PCE) is 0.07% . The Table below explain the photovoltaic performance results for both devices with and without gold plasmonic effect .

Device	$J_{sc}(\text{mA/cm}^2)$	$V_{oc}(\text{Volt})$	FF	PCE (%)	$I_m(\text{mA/cm}^2)$	$V_m(\text{Volt})$
Without gold	0.79	0.44	0.31179	0.07	0.47	0.1441
With gold	2.02	0.34	0.275	0.28	1.1	0.206

CONCLUSIONS

In brief, MWNT-PANI nanocomposite was prepared by using in chemical polymerization method and characterized by various techniques. A heterojunction solar cells comprising amorphous n-type silicon modified by gold nanoparticle and MWNT-PANI nanocomposite was fabricated. It was found that the in-situ polymerization process

can lead to effective site-selective interactions between the quinoid ring of the PANI and the MWNTs, which facilitate charge, transfer processes between the two components. The improved electronic properties in PANI due to the incorporation of MWNTs help to improve the solar cell performance. This study demonstrates that the MWNT-PANI composites are potential materials for fabricating low-cost solar cells. and another side we have fabricated (n-type Si/ gold particles/PANI-MWNTS) heterojunction solar cell, compared with same design without gold particle. The Au metal nanoparticles, which exhibit increase power conversion efficiency due to intense absorption by surface plasmon resonance in the visible region of the spectrum.

Acknowledgments

This work was supported Nanotechnology Center at University of Arkansas at Little Rock for using their facilities. SA gratefully acknowledges the scholarship support from Iraqi government.

REFERENCE

- [1]. Standridge, S.; Schatz, G.; and Hupp, J. *Langmuir* 2009, 25, 2596.
- [2]. Noginov, M. A.; Zhu, G.; Belgrave, A. M.; Bakker, R.; Shalaev, V. M.; Narimanov, E. E.; Stout, S.; Herz, E.; Suteewong, T.; Wiesner, U. *Nature* 2009, 460, 1110
- [3]. Schuller, J. A.; Barnard, E. S.; Cai, W. S.; Jun, Y. C.; White, J. S.; Brongersma, M. L. *Nat. Mater.* 2010, 9, 193–204.
- [4]. Atwater, H. A.; Polman, A. *Nat. Mater.* 2010, 9, 205.
- [5]. Ihara, M.; Tanaka, K.; Sakaki, K.; Honma, I.; Yamada, K. *J. Phys. Chem. B* 1997, 101, 5153.
- [6]. Service, R. *Science* 2008, 320 (5883), 1585.
- [7]. Pillai, S.; Catchpole, K. R.; Trupke, T.; Green, M. A. *J. Appl. Phys.* 2007, 101, No. 093105.
- [8]. Sarah, K.; Chul-Hyun, K.; Sang, L.; et al. *Chem. Commun.* 2013, 49, 6033–6035.
- [9]. Noginov, M. A.; Zhu, G.; Belgrave, A. M.; Bakker, R.; Shalaev, V. M.; Narimanov, E. E.; Stout, S.; Herz, E.; Suteewong, T.; Wiesner, U. *Nature* 2009, 460, 1110–1116
- [10]. Nakayama, K.; Tanabe, K.; Atwater, H. *Appl. Phys. Lett.* 2008, 93, No. 121904.
- [11]. Stuart, H.; Hall, D. *Phys. Rev. Lett.* 1998, 5663.
- [12]. Schaadt, D.; Feng, B.; Yu, E. *Appl. Phys. Lett.* 2005, 86, No. 063106.
- [13]. Hagglund, C.; Zach, M.; Kasemo, B. *Appl. Phys. Lett.* 2008, 92, No. 013113.
- [14]. Ishikawa, K.; Wen, C.; Yamada, K.; Okubo, T. *J. Chem. Eng. Jpn.* 2004, 37, 645.
- [15]. Rand, B.; Peumans, P.; Forrest, S. J. *Appl. Phys.* 2004, 96, 7519.
- [16]. Kulkarni, A. P.; Noone, K. M.; Munechika, K.; Guyer, S. R.; Ginger, D. S. *Nano Lett.* 2010, 10, 1501.
- [17]. Bach, U.; Lupo, D.; Comte, P.; Moser, J. E.; Weissortel, F.; Salbeck, J.; Spreitzer, H.; Gratzel, M. *Nature* 1998, 395, 583.
- [18]. Snaith, H. J.; Schmidt-Mende, L. *Adv. Mater.* 2007, 19, 3187.
- [19]. Standridge, S.; Schatz, G.; Hupp, J. *J. Am. Chem. Soc.* 2009, 131, 8407.
- [20]. Snaith, H. J.; Humphry-Baker, R.; Chen, P.; Cesar, I.; Zakeeruddin, S. M.; Gratzel, M. *Nanotechnology* 2008, 19, No. 424003.
- [21]. Wang, P.; Zakeeruddin, S. M.; Comte, P.; Exnar, I.; Gratzel, M. *J. Am. Chem. Soc.* 2003, 125, 1166.

- [22]. LizMarzan, L.; Giersig, M.; Mulvaney, P. *Langmuir* 1996, 12, 4329.
- [23]. Enustun, B. V.; Turkevich, J. *J. Am. Chem. Soc.* 1963, 85, 3317.
- [24]. Cerullo, G.; De Silvestri, S. *Rev. Sci. Instrum.* 2003, 74, 1.
- [25]. Liu, N.; Prall, B.; Klimov, V. *J. Am. Chem. Soc.* 2006, 128, 15362.
- [26]. Wu, D.; Xu, X.; Liu, X. *Solid State Commun.* 2008, 146, 7.
- [27]. Kelly, K. L.; Coronado, E.; Zhao, L. L.; Schatz, G. C. *J. Phys. Chem. B* 2003, 107, 668.
- [28]. Link, S.; El-Sayed, M. *J. Phys. Chem. B* 1999, 103, 8410.
- [29]. Ding, I. K.; Tetreault, N.; Brillet, J.; Hardin, B. E.; Smith, E. H.; Rosenthal, S. J.; Sauvage, F.; Gratzel, M.; McGehee, M. D. *Adv. Funct. Mater.* 2009, 19, 2431.
- [30]. Bhattacharyya, S.; Kymakis, E.; Amaratunga, G. A. *J. Chem. Mater.* 2004, 16, 4819.
- [31]. Chen, F.-C.; Wu, J.-L.; Lee, C.-L.; Hong, Y.; Kuo, C.-H.; Huang, M. H. *Appl. Phys. Lett.* 2009, 95, No. 013305.
- [32]. Pegg, L. J.; Schumann, S.; Hatton, R. A. *ACS Nano* 2010, 4, 5671.
- [33]. Westerling, M.; Vijila, C.; Osterbacka, R.; Stubb, H. *Phys. Rev. B* 2003, 67, No. 195201.
- [34]. Wenger, B.; Gratzel, M.; Moser, J. E. *J. Am. Chem. Soc.* 2005, 127, 12150.
- [35]. Jain, P. K.; Qian, W.; El-Sayed, M. A. *J. Phys. Chem. B* 2006, 110, 136.
- [36]. Tiwana, P.; Parkinson, P.; Johnston, M. B.; Snaith, H. J.; Herz, L. M. *J. Phys. Chem. C* 2010, 114, 1365.
- [37]. Wiley, B.; Chen, Y.; McLellan, J.; Xiong, Y.; Li, Z.; Ginger, D.; Xia, Y. *Nano Lett.* 2007, 7, 1032.
- [38]. Kumar, P. S.; Pastoriza-Santos, I.; Rodriguez-Gonzalez, B.; Garcia de Abajo, F. J.; Liz-Marzan, L. M. *Nanotechnology*
- [39]. Naoi, K.; Kawase, K.; Mori, M.; Komiyama, M. *Electrochemistry of Poly(2,2[prime]-dithiodianiline): A New Class of High Energy Conducting Polymer Interconnected with S Bonds.* *J. Electrochem. Soc.* 1997, 144, L173,.
- [40]. Shah, A. A.; Holze, R.; *In situ UV-vis spectroelectrochemical studies of the copolymerization of o-aminophenol and aniline.* *Synth. Met.* 2006, 156, 566.
- [41]. Chen, C.; Sun, C.; Gao, Y. *Electrosynthesis of poly(aniline-co-p-aminophenol) having electrochemical properties in a wide pH range.* *Electrochim. Acta* 2008, 53, 3021.
- [42]. Bauhofer, W.; Kovacs, J. Z. *A review and analysis of electrical percolation in carbon nanotube polymer composites.* *Compos. Sci. Technol.* 2008, 69, 1486.
- [43]. Blanchet, G. B.; Fincher, C. R.; Gao, F. *Polyaniline nanotube composites: A high-resolution printable conductor.* *Appl. Phys. Lett.* 2003, 82, 1290.
- [45]. Konyushenko, E. N.; Prokes, J.; Cieslar, M.; Hwang, J. Y.; Chen, K. H.; Sapurina, J. *Polymer* 2006, 47, 5715.